Journal of the European Ceramic Society **18** (1998) 1293–1299

PII: S0955-2219(98)00056-9
0955-2219/98/$—see front matter

Thermal Oxidation Under Oxygen of Zirconium Nitride Studied by XPS, DRIFTS, TG-MS

Hugues Wiame,* Miguel-Angel Centeno,† Sandra Picard, Philippe Bastians and Paul Grange

Université catholique de Louvain, Unité de Catalyse et de Chimie des Matériaux Divisés, 2, Place Croix du Sud bte17, 1348 Louvain-la-Neuve, Belgium

Abstract

The studies of oxidation of nitrides or oxynitrides compounds are important since their electrical, thermal, catalytical and reactional properties are drastically modified by the oxidation layer encountered on top of these ceramics. In this paper we present the thermal oxidation of ZrN under O_2, in order to have a better understanding of the intermediate species encountered during the reaction, in the frame of low temperature nitridation of ceramics. The analysis of gas reaction products during oxidation and the confrontation of XPS and DRIFTS results on partially oxidized samples allow to evidence the formation of a stable Zr–N–N–O–Zr intermediate. © *1998 Elsevier Science Limited. All rights reserved*

1 Introduction

Nitride and oxynitride refractory ceramics are very attractive compounds because of their mechanical, thermal, electrical and catalytical properties. AlN for example possesses a high electrical resistivity, a good thermal conductivity and stability up to very high temperatures as well as a thermal expansion coefficient which is close to that of silicon.[1,2] These properties make it very interesting for microelectronic devices. TiN combines characteristics of both covalent compounds, such as extreme hardness and high melting point, and of metallic compounds such as good thermal and electrical conductivity.[3,4] TiN is extensively used in cutting tools and by coating industries. Furthermore, it has been found to form excellent diffusion barriers and to be impermeable to Si atoms in metallization schemes to silicon semiconductor devices.[5]

Concerning catalytic activity of nitrides, molybdenum nitride[6] is known to be active in dehydronitrogenation of pyridine and on the AlPON oxynitride catalysts, Massinon have shown that the substitution of oxygen by nitrogen during nitridation induces basic surface properties.[7] Properties of other nitrides such as ZrN have also been reviewed.[8]

Although nitrides are thermodynamically stable, they are readily oxidized even at room temperature.[9,10] This oxidation or contamination by oxygen can be a major problem (or can be intentional, i.e. passivation of samples) since it completely modifies the properties and reactivities of those solids. In this paper, the thermal oxidation of ZrN is studied. It is followed by ThermoGravimetry on line Mass Spectroscopy (TG-MS), X-ray Photelectron Spectroscopy (XPS) and Diffuse Reflectance Infrared Fourier Transform Spectroscopy (DRIFTS). The purpose of this study is to have a better understanding of the oxidation–nitridation mechanism since low temperature nitridation reactions are of interest to reduce the production cost of these materials.[11]

Oxidation of nitrides and study of their stability have mainly concerned TiN,[5,6,10–13] and AlN,[9,14,15] only few papers have been published on stability and oxidation of ZrN.[16] Nevertheless, it seems that oxidation of nitrides proceeds in the same way on all these compounds. During oxidation, the oxygen substitutes the nitrogen which leaves the solids as gaseous N_2. Before complete oxidation occurs, an intermediate step is generally observed. During this step, nitrogen is characterized by the binding energy (BE) of the N1s peak, determined by XPS, that varies between 401·5 and 403·5 eV whatever

*To whom correspondence should be addressed.
†On leave from Departamento de Quimica Inorganica e Instituto de Ciencia de Materiales de Sevilla, Universidad de Sevilla-CSIC, PO, Box 874, 41071 Sevilla, Spain.

the metal. The interaction of this nitrogen with the solid is not always described in the same way. Wang and co-workers[15] attribute this N1s peak to a N–O bonding either within the growing oxide layer or at the Al_2O_3/AlN interface. For this species, stable at elevated temperature, Legendre[13] proposes a M–N = N–M type structure very similar to what is found in titanium dinitrogen complexes in organometallic chemistry. By sputtering of TiO_2 by nitrogen or argon, Wolff *et al.*[17] has suggested that part of N_2 is trapped in the solid. This 'dissolved' N_2 species accumulates and then reacts with the oxide to form titanium oxynitride. This nitridation process occurs only after the sputtering of a certain amount of oxygen. Furthermore, analysing the XPS binding energy shift of N1s, in the N_2 form, as a function of the average binding energy of $Ti_{2p3/2}$, they assumed a strong interaction of N_2 with its environment since a 1·2 eV shift (from 402·3 to 403·5 eV) was observed when Ti $2p_{3/2}$ binding energy shifted from 458·8 to 458·1 eV. The same trend was observed for dissolved Ar when TiO_2 was reduced to Ti and this was attributed to the position of Ar which occupies some octahedral or tetrahedral holes in the oxygen sublattice. Legendre[13] shows exactly the same behaviour when oxygen content increases the N1s peak shift to higher binding energy. An other important feature is presented by Milosev *et al.*[18] when, by oxidation of TiN to TiO_2, he observed by XPS an intermediate step characterized by a N_2 dissolved species, as observed by Wolff in the nitridation process of TiO_2 to TiON. This allows us to conclude that the oxidation–nitridation process is reversible and that the intermediate, a strongly interacting N_2, is identical.

2 Experimental

The ZrN used in this work was synthesized by carbothermal nitridation from a mixture of ZrO_2 and active carbon. ZrO_2 was synthesized by a sol–gel method. The stoechiometry introduced for nitridation reaction was C/ZrO_2 = 0·5. The nitridation was realized in a tubular oven under high NH_3 electronic grade flow. The rate of heating was controlled at 10 K min^{-1} up to 1573 K, temperature which was maintained for 15 h. The pure ZrN phase was confirmed by X-ray diffraction. Chemical analysis revealed the presence of 3 wt% of residual carbon coming from the synthesis.

The weight change of the ZrN powder during oxidation was monitored using a SETARAM TG_DTA 92 electro-balance connected on line with a mass spectrometer. 20 mg of sample was heated in an alumina crucible under a O_2/He (5/95) flow of 125 ml min^{-1} at a constant rate of 5 K min^{-1} from room temperature up to 1173 K. The mass range scanned varied from 10 to 70 m/e.

The ZrN samples studied by XPS and DRIFTS were oxidized before analysis by heating 100 mg of powder in a U type reactor under O_2/He (5%/95%) 50 ml min^{-1} flow. The heating rate was programmed at 3 K min^{-1} up to 773 and 1073 K.

The XPS analysis were performed with an SSI X-Probe (SSX-100/206) photoelectron spectrometer, equipped with a monochromatized microfocus Al X-ray source, a 30° solid angle acceptance lens, a hemispherical analyser and a position sensitive detector. The sample powders pressed in small stainless steel troughs of 4 mm diameter were placed on a ceramic carousel. Due to their semiconductor character the samples undergo a differential charging effect[19] when they are deposited on a conductive carousel. This provokes broadening, distortion, or even splitting of peaks which can be confused with a chemical shift effect. The differential charging effect can be avoided by mounting the sample on an insulating home made ceramic carousel (Macor® Switzerland), with the nickel grid, mentioned below, still grounded to the carousel support. The carousel is placed in the introduction chamber of the spectrometer. The samples were heated by a quartz lamp (max 393 K) three times 15 min under vacuum, heating periods were separated by 30 min outgassing. The samples were then outgassed overnight under vacuum and introduced in the analysis chamber. The pressure in the analysis chamber was around 10^{-7} Pa. The angle between the surface normal and the axis of the analyser lens was 55°. The spot size was approximatively 1·4 mm^2 and the pass energy was set at 50 eV. In these conditions, the resolution determined by the full width at half maximum (FWHM) of the $Au_{4f7/2}$ peak of a standard gold sample was around 1·1 eV. A flood gun set at 10 eV and a Ni grid placed 3 mm above the sample surface were used for charge compensation. The following sequence of spectra was recorded, survey spectrum, C1s, Zr3d, O1s, N1s, and C1s again to check the absence of degradation of the sample during the analysis. The binding energies were calculated with respect to the C–(C,H) component of the C1s adventitious carbon fixed at 284·8 eV. The spectra were decomposed with the least squares fitting routine provided by the manufacturer with a Gaussian/Lorentzian ratio of 85/15 and after substraction of a linear baseline. The Zr 3d5/2/3d3/2 area ratio was imposed to the theorical value of 0·66 and the interval between components was fixed at 2·43 eV. The atomic concentration ratios were calculated using peak areas normalized on the basis of acquisition parameters and sensitivity

factors provided by the manufacturer (mean free path varying according to the 0·7th power of the photoelectron kinetic energy; Scofield cross sections; transmission function assumed to be constant).

In-situ DRIFTS spectra were obtained in a Bruker IFS 88 spectrometer with a DTGS detector using a temperature and environment controlled chamber (Spectra-Tech 0030-103). Preoxidized samples without any dilution were placed in the DRIFTS cell and spectra were recorded at room temperature in the 400–4000 cm^{-1} range with 4 cm^{-1} resolution. In order to evaluate the thermal stability of our sample, another spectra was taken after 2 h in nitrogen flow (30 ml/min^{-1}) at 723 K. The spectra of an aluminium mirror was used as background. Since ZrN is a black powder, the sample was diluted in KBr (1/20) before recording at RT. In that case the KBr spectra was used as background.

3 Results and discussion

Figure 1 presents the weight change observed when ZrN is oxidized at 5 K/min under oxygen atmosphere. The weight gain begins slowly from 573 to 773 K and then a sharp increase is observed up to 923 K. After that, the oxidation slows down and an overweight region from what is expected for complete oxidation of ZrN into ZrO_2, between 923 and 973 K, is observed. In Fig. 2, oxidation is achieved in dry air at a heating rate of 1 K min^{-1} between 748 and 1173 K. The overweight is even more pronounced proving that it was not a diffusionnal nor a kinetic artefact. This behaviour has already been observed by Legendre[13] on thermal oxidation of TiN. He explains that part of the N_2 produced by the reaction $TiN + O_2 = TiO_2 + 1/2N_2$ is caught under a M–N = N–M structure before leaving the solid at a higher temperature, this N_2 should be responsible for the weight excess.

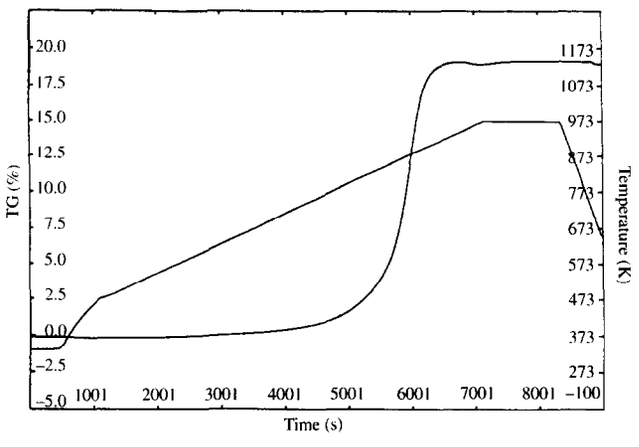

Fig. 1. ATG curve of oxidation of Zirconium Nitride under O_2/He (5%/95%). 5 K/min^{-1} heating rate is maintained constant from 473 to 973 K.

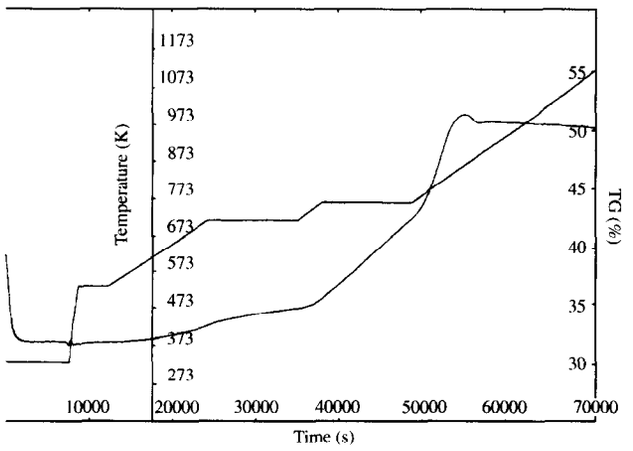

Fig. 2. ATG curve of oxidation of ZrN under dry air. 1 K min^{-1} heating rate is maintained constant from 748 to 1173 K.

Figure 3 shows mass-spectroscopy results for ZrN oxidation presented in Fig. 1 in the 723 and 973 K range. The m/e 12, 14, 28, 30, 32 and 44 can be attributed to 'C', 'N', 'N_2 or CO', 'NO', 'O_2' and 'CO_2 or N_2O', respectively. Carbon and nitrogen are due to the fragmentation of carbonated or nitrogenated species when these species are ionized in the mass spectrometer. N_2, NO and CO can be due to either oxidation reaction products or fragmentation of ionizing N_2O or CO_2. The reaction products of the oxidation of zirconium nitride are: N_2 as expected if the oxidation reaction proceeds by $ZrN + O_2 = ZrO_2 + 1/2\ N_2$, CO_2 and CO as expected since the ZrN powder is not free of carbon. In addition, NO (m/e 30) and a small quantity of N_2O (m/e 44) are detected. The presence of N_2O was proved by oxidation of pure zirconium nitride where m/e 44 can only be assigned to nitrogen containing molecules since no C (m/e 12) was found. The O_2 consumption associated to products formation presents a sharp minimum when the weight gain is the quickest and when all products curves pass through a maximum.

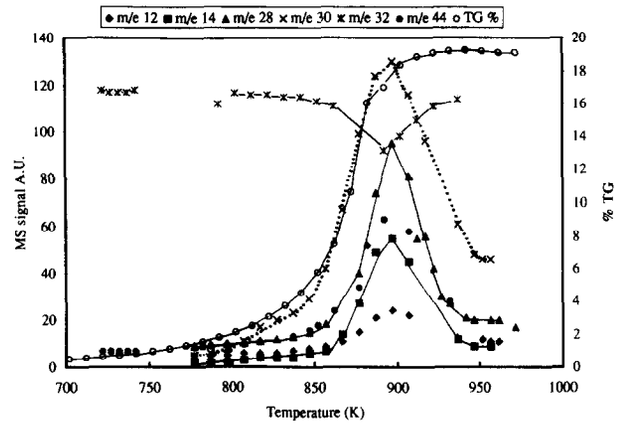

Fig. 3. Mass-spectroscopy analysis of the gas reaction products of ZrN thermal oxidation (Fig. 1) under O_2/He (5%/95%). m/e 12 and 14 are fragmentation carbon and nitrogen, m/e 28, 30, 44 are assigned to N_2–CO, NO, N_2O–CO_2.

XPS spectra of Zr_{3d}, N_{1s} and O1s of ZrN, ZrN oxidized at 823 and 1173 K and commercial ZrO_2 are presented in Figs 4–6. The spectra presented here correspond quite well to those obtained by Milosev *et al.*[16] Since no special care was taken to prevent surface oxidation of ZrN, an oxide layer is present. The Zr 3d peak has been decomposed in two 3d doublet. The Zr $3d_{5/2}$ component at 182·2 eV is close to 182 eV observed in ZrO_2 and the component at 180·3 eV corresponds to Zr-N. No oxynitride peak are necessary to describe the experimental spectrum contrary to what was observed by Milosev *et al.*[16] who presented a peak at 182·2 eV for the oxynitride (ZrO_2 is at 183·1 eV). Nevertheless, in our samples, the Full Width at Half Maximum of the component Zr $3d_{5/2}$ attributed to Zr–O is 2·3 eV, while the width of the Zr $3d_{5/2}$ in commercial ZrO_2 is 1·4 eV; so the presence of ZrON can be suspected. Heating the sample at 823 and 1173 K under oxygen causes the Zr–N contribution to disappear.

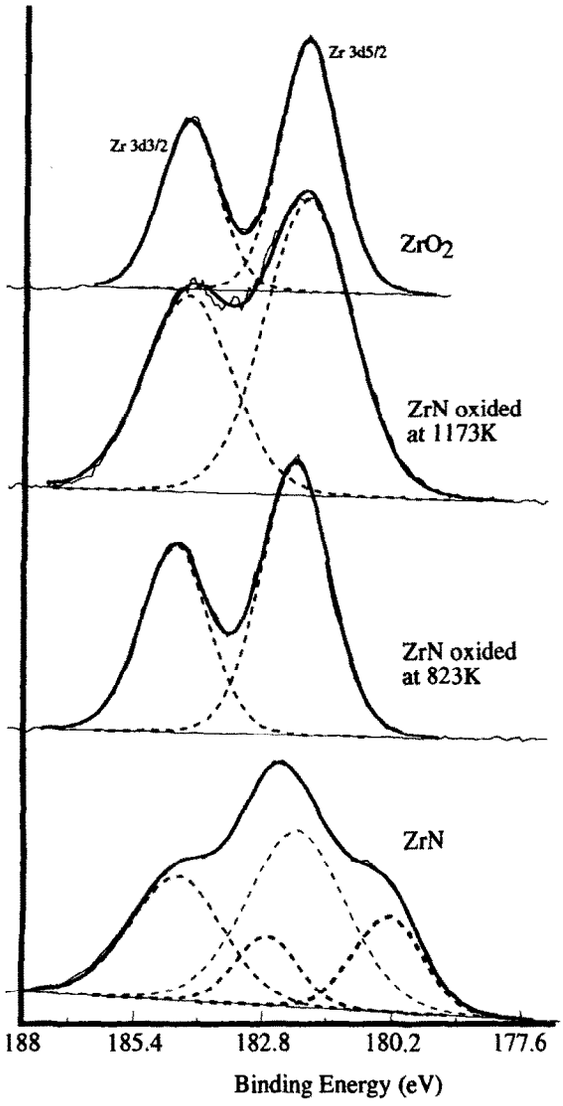

Fig. 4. Zr3d XPS spectra of ZrN, ZrN oxidized at 823 and 1173 K, commercial ZrO_2.

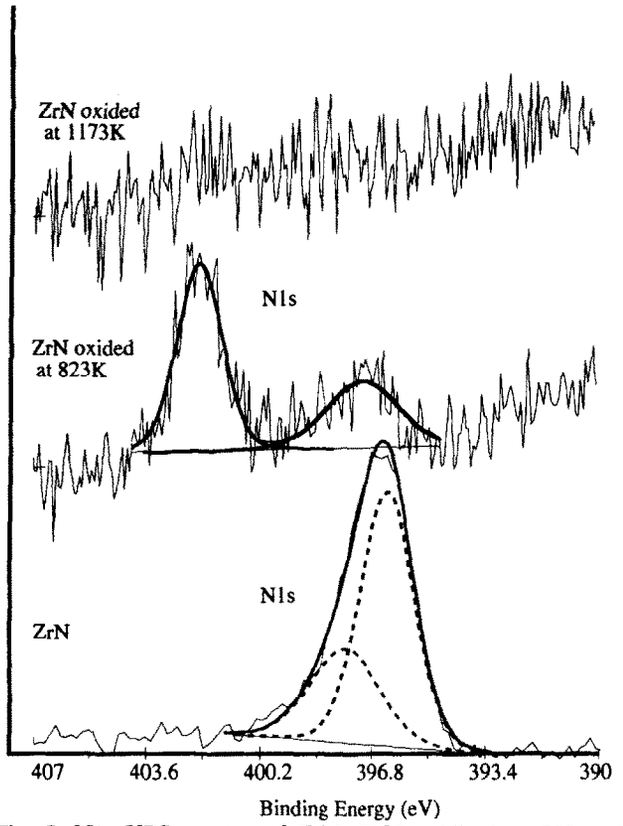

Fig. 5. N1s XPS spectra of ZrN, ZrN oxidized at 823 and 1173 K.

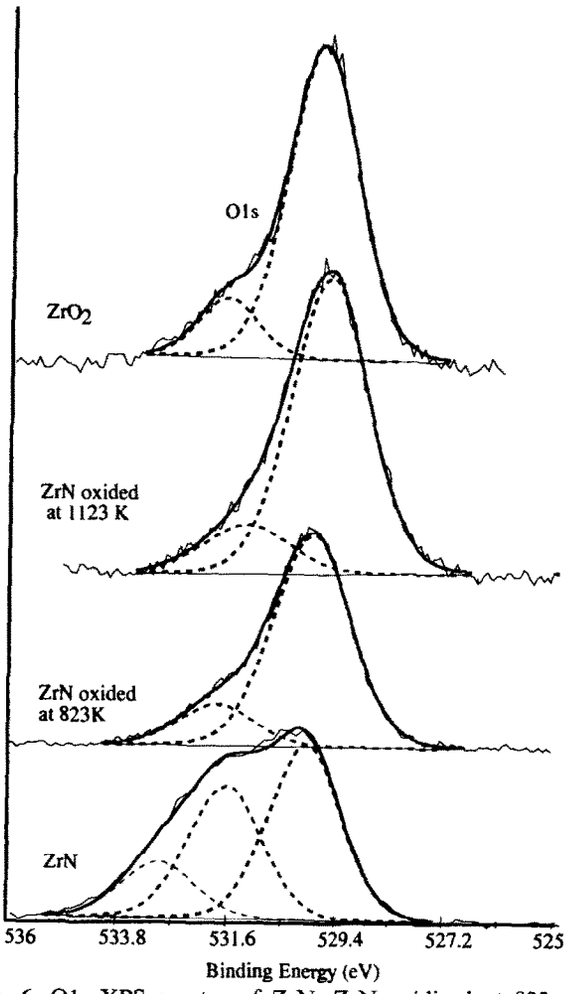

Fig. 6. O1s XPS spectra of ZrN, ZrN oxidized at 823 and 1173 K, commercial ZrO_2.

The N1s peak of ZrN can be decomposed in two components, one at 397·8 eV and one at 396·6 eV. Both peaks are observed by Milosev *et al.*[16] The first one is attributed to the nitride in Zr–N The second one at 396·6 eV corresponds to a nitride N^{3-} in ZrON oxynitride. Oxidation of ZrN up to 823 K leads to a drastic change in the N1s profile. The nitride contribution decreases and a high binding energy peak appears centered at 402·8 eV. This peak is attributed by most authors to a dinitrogen species dissolved in the solid and in strong interaction with the solid. At higher temperature, no N1s signal is observed. The position of the oxygen O1s peak located at 530 eV confirms the presence of ZrO_2 and shows that OH groups (BE = 531·9 eV) and water (BE = 533·1 eV) are adsorbed on the ZrN. The latter species are removed by heating.

DRIFTS spectra are presented in Figs 7 and 8. Figure 7 presents the spectra obtained when ZrN is oxidized at increasing temperature. The spectra is characterised by a strong absorbtion at 773 cm^{-1} for samples oxidized at 823 K which correspond to the structure vibration Zr–N, Zr–O. When increasing the oxidation temperature, this band shift to 830 cm^{-1} and corresponds to ZrO_2,[20] showing a progressive substitution of nitrogen by oxygen since on ZrN fresh sample absorption is centered at 750 cm^{-1} (not shown here). This substitution mainly occurs in the bulk and not on the surface since XPS results has evidenced a completely oxidized surface for all the oxidation temperature. In addition, bands in the 1200–1740 cm^{-1} range are observed. They are attributed to carbonate and formate species formed on the surface of the solid during the oxidation of residual carbon.[21] The same bands appear on ZrO_2 prepared by sol–gel method and calcined at 1173 K under air and are stable under inert atmosphere at 723 K.

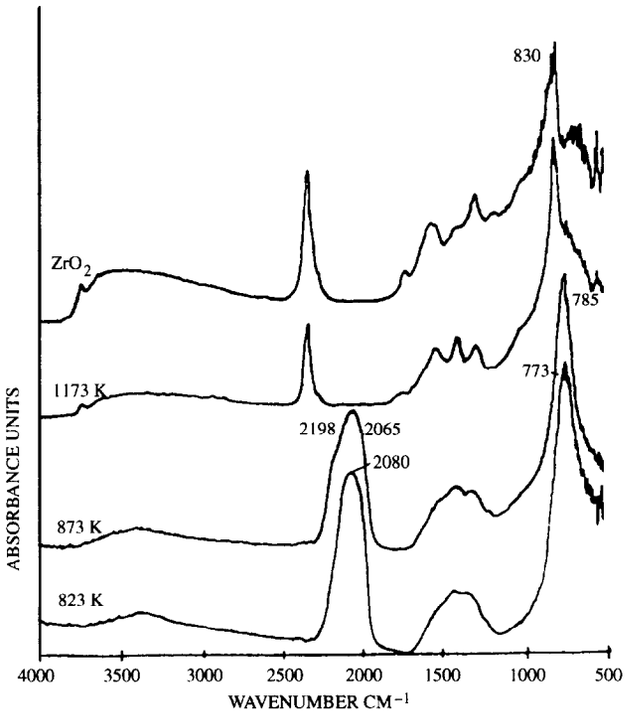

Fig. 7. DRIFTS sprectra of ZrN oxidized at 823 K, ZrN oxidized at 873, 1173 K, and ZrO_2.

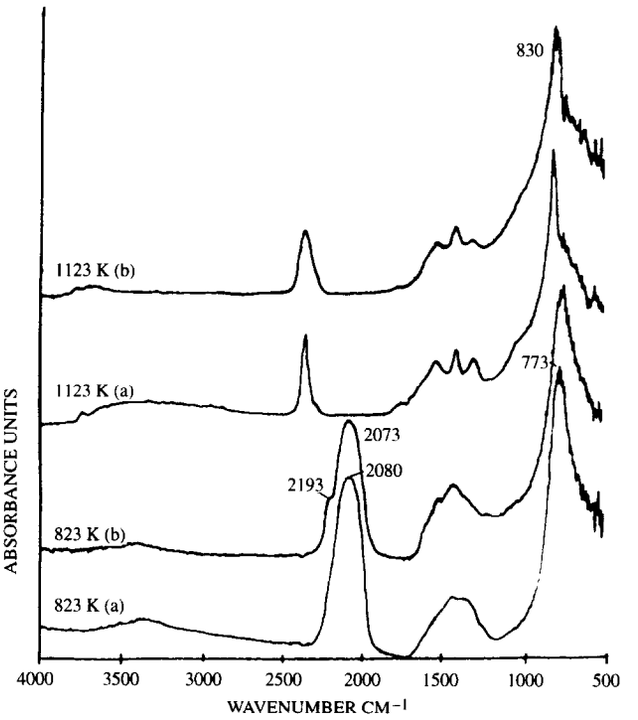

Fig. 8. DRIFTS sprectra of ZrN oxidized at (a) 823 K, and (b) oxidized at 823 K and heated under N_2 at 773 K (a) ZrN oxidized at 1123 K spectrum at RT, and (b) spectrum taken at 773 K under N_2.

A very intense vibration band appears at 2080 cm^{-1} on the 823 K oxidized ZrN powder. When the temperature is raised up to 873 K, a shoulder appears at 2198 cm^{-1} and the main peak shifts to a lower wavenumber (2065 cm^{-1}). The same behaviour is observed on the 823 K oxidized sample when heated at 723 K under nitrogen (Fig. 8). Since these bands are still present at such a high temperature, they should not correspond to adsorbed species. By raising the temperature up to 1173 K, these bands disappear and a ZrO_2 like structure is observed. The same vibrations have been recently observed by Baraton *et al.*[22] on aluminium nitride powder and by Liu *et al.*[23] on AlN thin films. They have also been observed on other nitrides and oxynitrides obtained by 'clean' synthesis without carbon and are attributed to nitrogenated species and not to adsorbed CO species.

Gas analysis by mass spectroscopy showed that oxidation reaction products are N_2, NO, N_2O for nitrogenated compounds and small amounts of CO and CO_2 due to residual active carbon introduced during synthesis. XPS data of oxided ZrN present an intermediate step where the nitride has nearly completely disappeared and where a high energy

species increases before complete N1s signal depletion. The temperature at which this peak is detected coincides with that observed for the detection of the DRIFTS vibration located at 2080 cm^{-1}. This N1s species, at a binding energy of 402·8 eV, is generally attributed to M–N_2 interaction and not to a NO or N_2O because no corresponding N–O O1s peak around 533 eV representing molecular NO is observed. It is interesting to keep in mind that dissociative NO adsorption leads to the formation of a N1s species around 397 eV and of an O1s species at 530 eV.[24]

The 2125 cm^{-1} DRIFTS vibration has been assigned to Al–NN by Liu *et al.*[23] because he observed an associated XPS N1s peak at 400·8 eV. This attribution was not supported by Baraton *et al.*[22] who observed, on the same compound, a similar vibration at 2157 cm^{-1} but no XPS N1s signal in the 400–403 eV range. Furthermore, hydrogen–deuterium exchange has no effect on this stretching vibration, proving that it is not an Al–H bond.[22] Taking these results into account we propose that the 2198 cm^{-1} vibration we evidenced is due to a nitrogen–oxygen interacting species ($NO^{\delta+}$ or N_xO_y) in the solid since the intensity of this band increases with the oxidation state, in particular the temperature of oxidation. The same behaviour is observed for the band located at 2065 cm^{-1}. In order to explain the presence of N_2 in the reaction products and the XPS N1s binding energy at 402·7 eV, we could attribute the vibration centered on 2065 cm^{-1} to M–N_2–M species. The same band is observed by Oh-Kita *et al.*[25] for strongly adsorbed N_2 on metal alumina catalyst.

Furthermore, this intermediate species has been shown by several authors to be thermally stable and in strong interaction with the solid. Its XPS binding energy is shifted to higher values when more oxygen is incorporated into the nitride. Since a small quantity of N_2O was detected in our oxidation reaction products, we explain all these results by the formation, during the oxidation process, of an intermediate such as: Zr–N–N–O–Zr. A similar intermediate has been reported in the literature for the reduction of NO by NH_3[26] and can be easily understood taking into account the very lacunary structure encountered on ZrN and already proposed and illustrated as follows (Fig. 9) by Gilles.[27]

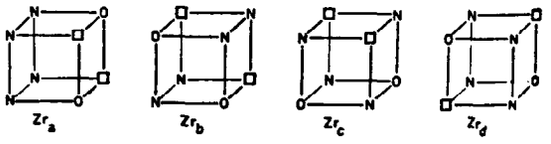

Fig. 9. Zirconium oxynitride structure proposed by Gilles.[27]

Thus the oxidation process can be written as follow:

$$ZrN + O_2 \Longleftrightarrow Zr - N - N - O - Zr \Longleftrightarrow ZrO_2$$

This intermediate can explain the observation of N_2, NO, and N_2O in the reaction products on TG-MS during oxidation. It also explains the absence of any O1s at 533 eV binding energy (NO adsorbed molecule) since oxygen occupies a position similar to that found in a metal oxide with an expected XPS binding energy of 530 eV (metal oxide interaction). Nevertheless, since NO is present in the gaz phase, it must be conclude that it desorbed readily in the gaz phase after synthesis and that no reabsorption of this NO occurs on the ZrN at this temperature of reaction (823–1123 K). The proposed species are responsible for the N1s peak (BE = 403 eV) evidenced by XPS and both the 2065 and 2198 cm^{-1} DRIFTS bands observed by DRIFTS.

Acknowledgements

The authors thank the Belgian 'Région Wallonne' for financial support.

References

1. Sheppard, L. M., Aluminium nitride: a versatile but challenging material. *Am. Ceram. Soc. Bull.*, 1990, **69**(11), 1801–1812.
2. Ponthieu, E., Lonnay, L., Leclercq, L., Bechara, R., Grimblot, G., Grange, P. and Delmon, B., Proposal of a composition model for commercial AlN Powders. *Journal European Ceramic Society*, 1991, **8**(1), 233–241.
3. Kamiya, K., Yoko, T. and Bessho, M., Nitridation of TiO_2 fibres prepared by the Sol–gel Method. *J. Mat. Sci.*, 1979, **14**, 70–80.
4. Tompkins, H. G., Oxidation of titanium nitride in room air and dry O_2. *J. Appl. Phys.*, 1991, **70**, 3876–3880.
5. Wittner, M., Noser, J. and Melchior, H., Oxidation kinetics of TiN films. *J. Appl. Phys.*, 6659, **52**(11), .
6. Colling, C. W., Choi, J.G. and Thompson, L., Molybdenum nitride catalysts: H_2 temperature programmed reduction and NH_3 temperature programmed desorption. *J. Catal.*, 1996, **160**, 35–42.
7. Massinon, A., Odriozola, J. A., Bastians, Ph., Conanec, R., Marchand, R., Laurent, Y. and Grange, P., Influence of nitrogen content on the acid-base properties of aluminophosphate oxynitrides. *Appl. Catal. A*, 1996, **137**, 9–23.
8. Toth, L.E., *Transition Metal Carbides and Nitrides*. Academic Press, New York, 1971.
9. Katnani, A. D. and Papathomas, K. I., Kinetics and initial stages of oxidation of aluminium nitride: Thermogravimetric analysis and x-ray photoelectron spectroscopy study. *J. Vac. Sci. Technol.*, 1987, **A5**(4), 1335–1340.
10. François, J. C., Massiani, Y., Gravier, P., Grimblot, J. and Gengembre, L., Characterization and optical properties of thin films formed on TiN coatings during electrochemical treatments. *Thin Solid Films*, 1993, **223**, 223–229.
11. Clement, F., Bastians, P. and Grange, P., Novel low temperature synthesis of titanium nitride: a proposal for cyanonitridation mechanism. *J. Solid States Ionic*, in press.

12. Saha, N. C. and and Tompkins, H. G., Titanium nitride oxidation chemistry: an x-ray photoelectron spectroscopy study. *J. Appl. Phys.*, 1992, **72**(7), 3072–3079.
13. Legendre, L., Marchand, R., Laurent, Y. A new class of inorganic compounds containing dinitrogen–metal bonds. *Journal European Ceramic Society* in press.
14. Nicolaescu, I. V., Tardos, G. and Riman, R. E., Thermogravimetric determination of carbon, nitrogen, and oxygen in aluminium nitride. *J. Am. Ceram. Soc.*, 1994, **77**(9), 2265–2272.
15. Wang, P. S., Malghan, S. G. and Hsu, S. M., The oxidation of aluminium nitride powder studied by bremsstrahlung-exited Auger electron spectroscopy and x-ray photoelectron spectroscopy. *J. Mater. Res.*, 1995, **10**(2), 302–305.
16. Milosev, I., Strehblow, H. H., Gaberscek, M. and Navinsek, B., Electrochemical oxidation of the ZrN hard (PVD) coatings studied by XPS. *Surf. and Interf. analysis*, 1996, **24**, 448–458.
17. Wolff, M., Schultze, J. W. and Strehblow, H. H., Low-energy implantation and sputtering of TiO_2 by nitrogen and argon and the electrochemical reoxidation. *Surf. and Interf. Anal.*, 1991, **17**, 726–736.
18. Milosev, I., Strehblow, H. H., Navinsek, B. and Metikos-Hukovic, M., Electrochemical and thermal oxidation of TiN coatings studied by XPS. *Surf. and Interf. Anal.*, 1995, **23**, 529–539.
19. Barr, T. L., *Modern ESCA, the Principles and Practice of X-ray Photoelectron Spectroscopy* CRC Press, Boca Raton, FL, 1993.
20. Lin, J., Chen, H. Y., Chen, L., Tan, K. L. and Zeng, H. C., N_2O decomposition over ZrO_2–an in situ DRIFT, TPR, TPD and XPS study. *Appl. Surf. Sci.*, 1996, **103**, 307–314.
21. Morterra, C., Orio, L. and Emanuel, C., Infrared spectroscopic surface characterization of zirconium oxide. Part 3— The CO/CO_2 and CO/H2O interactions at the surface of a high area monoclinic preparation. *J. Chem. Soc. Faraday Trans.*, 1990, **86**(17), 3003–3013.
22. Baraton, M. I., Chen, X. and Gonsalves, K. E., FTIR analysis of the surface of nanostructured aluminium nitride powder prepared via chemical synthesis. *J. Mater. Chem.*, 1996, **6**(8), 1407–1412.
23. Liu, H., Bertholet, D. C. and Rogers, J. W., Reactions of trimethylaluminium and ammonia on alumina at 600 K—surface chemical aspects of AlN thin film growth. *Surface Science*, 1995, **340**, 88–100.
24. Schreifels, J. A., Deffeyes, J. E., Neff, L. D. and White, J. M., An X-ray Photoelectron Spectroscopy Study of the Adsorption of N_2, NH_3, NO, N_2O on Dysprosium. Elsevier Scientific, Amsterdam, 1982, pp 190–209.
25. Oh-Kita, M., Aika, K., Urabe, K. and Ozaki, A., Infrared active adsorbed nitrogen on alkali metal-promoted transition metal–alumina catalyst. *J. Catal.*, 1976, **44**, 460–466.
26. Topsoe, N. Y., Dumesic, J. A. and Topsoe, H., Vanadia/titania catalysts for selective catalytic reduction of nitric oxide by ammonia. *J. Catal.*, 1511995, **241–252**, .
27. Gilles, J. C., Preparation par reaction à l'etat solide et structures des oxynitrures de zirconium. Mémoire présenté à la société chimique française, pp. 2118–2122, 1962.